RSC Advances

ROYAL SOCIETY OF CHEMISTRY

www.rsc.org/advances

Journal Name

RSCPublishing

COMMUNICATION

Homogeneous growth of conducting polymer nanofibers by electrodeposition for superhydrophobic and superoleophilic stainless steel meshes

Cite this: DOI: 10.1039/x0xx00000x

Received 00th January 2012,
Accepted 00th January 2012

DOI: 10.1039/x0xx00000x

www.rsc.org/

Thierry Darmanin and Frédéric Guittard*

Superhydrophobic and superoleophilic stainless steel meshes are produced by homogeneous formation of nanofibers around the mesh wires. The nanofibers are obtained by electrodeposition of poly(3,4-propyledioxythiophene) bearing two linear or branched hydrocarbon chains.

1. Introduction

The superhydrophobicity is a major field of research in a theoretical point of view[1-2] and for their resulting potential applications such as in anti-icing and anti-corrosion coatings, sensors, catalyses, batteries, optical devices, microfluidics, anti-bacteria, repellent textiles or oil/water separation.[3-5] The formation of superhydrophobic materials needs the creation of surface structures, as shown by the Wenzel[6] and Cassie-Baxter[7] equations and natural species.[8]

Many processes can be used to induce the formation of surface structures.[9] Among them, the electrodeposition of conducting polymers is a fast and easy process with the possibility to tune the surface morphology and roughness by changing the electrochemical parameters or the monomer structure.[10-12] The surface hydrophobicity can be controlled using hydrophobic doping agents or by introducing hydrophobic substituents.[10] The formation of nanofibers is highly specific to the monomer structure and they can be obtained using aniline,[13] pyrrole,[14] 3,4-ethylenedioxythiophene (EDOT)[15,16] or 3,4-propylenedioxythiophene (ProDOT) derivatives.[17-21] ProDOT is a key heterocycle due to exceptional polymerization capacity and the control of nanofiber formation with the substituent hydrophobicity, size and position.[17,20,21]

To enhance the superhydrophobic properties, meshes can be used as textured surfaces.[22-24] The presence of the mesh texture and nanostructures such as nanofibers around the mesh wires are ideal to produce meshes for oil/water separation.[25,26] Due to their complex geometry, the surface modification of textured surfaces such as meshes is easier using processes able to induce the formation of surface structures from the surface. The electrodeposition is one of the methods. For the fabrication of meshes for oil/water separation, three strategies were developed in the literature: superhydrophobic and superoleophilic meshes,[25,26] superhydrophilic and underwater superoleophobic meshes,[27,28] and more rarely superhydrophilic and superoleophobic meshes.[29] In the case of superhydrophobic and superoleophilic meshes, the best route is the use materials with hydrophobic and oleophilic properties such as hydrocarbon derivatives.

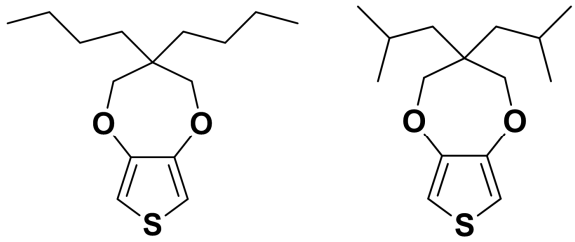

ProDOT-*n*-F$_4$ **ProDOT-*br*-F$_4$**

Scheme 1 Monomers used in this work.

Here, we report the formation of superhydrophobic and superoleophilic meshes by electropolymerization of the two monomers, represented in Scheme 1 and bearing two linear or branched hydrocarbon chains, in order to produce homogeneous nanofibers around the mesh wires. These monomers were used for their ability to form nanofibers.

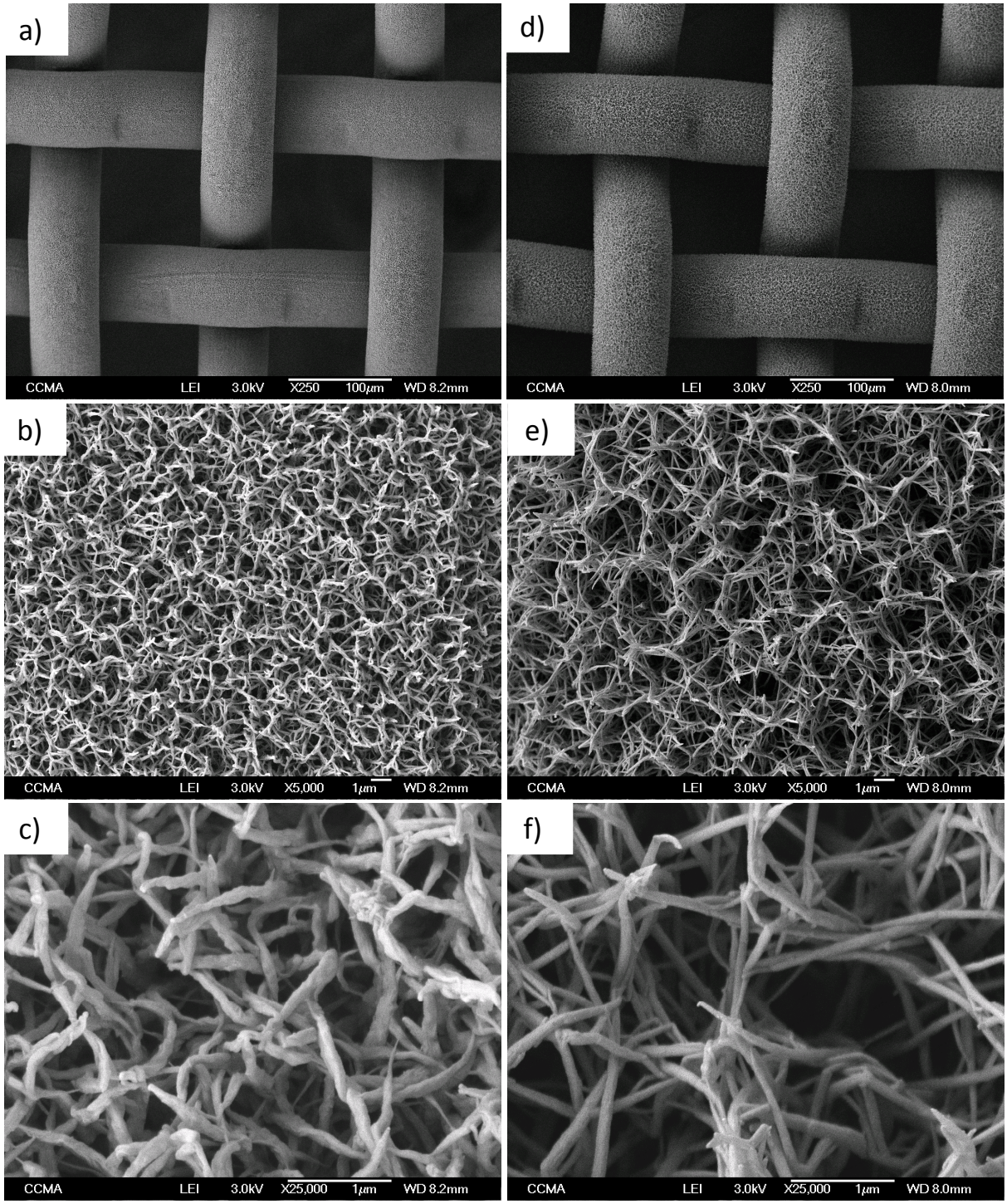

Fig. 1 SEM images at different magnifications of (a-c) PProDOT-*n*-H_4 and (d-f) PProDOT-*br*-H_4 electrodeposited on stainless steel meshes; Number of deposition scans: 3.

The surface properties of the modified meshes were analysed by contact angle measurement and scanning electron microscopy (SEM). The influence of the monomer structure and the number of deposition scans (deposition by cyclic voltammetry) are also reported.

2. Experimental

2.1 Electrodeposition

The monomers ProDOT-*n*-H_4 and ProDOT-*br*-H_4 were synthesized using a procedure reported in the literature.[17,20]

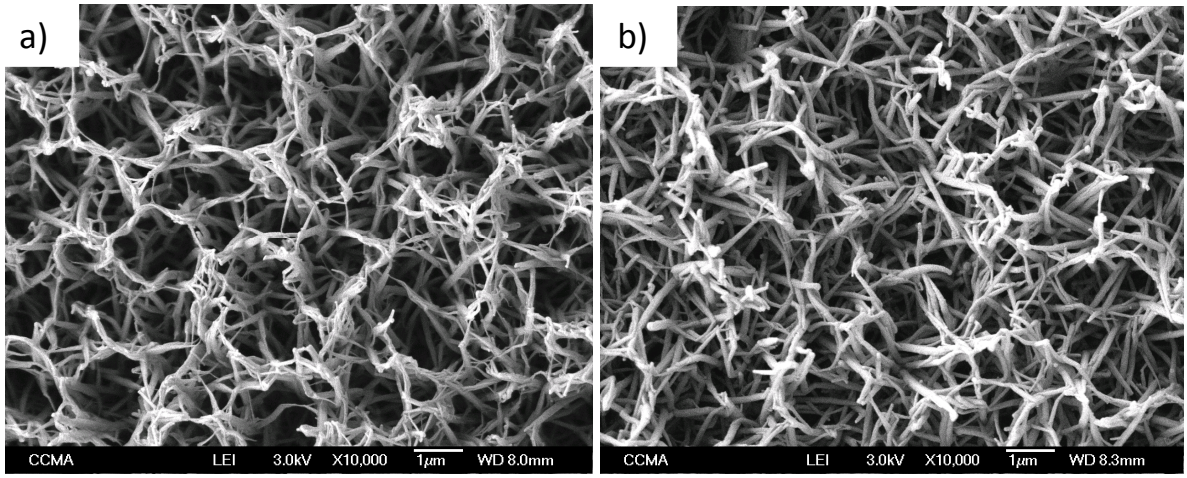

Fig. 2 SEM images PProDOT-*br*-H_4 electrodeposited on stainless steel meshes after (a) 1 deposition scan and (b) 10 deposition scans; Magnification: x10000.

The deposition were performed on stainless steel meshes (opening 100 μm; Fisher Bioblock) in two electrodeposition steps. The first step consisted in an electrodeposition of a smooth polypyrrole film in order to enhance the adherence of the films and to reduce the oxidation potential of the ProDOT monomers. In a glass electrochemical cell were put 0.25 M of pyrrole and 0.08 M of oxalic acid in deionized water. Three electrodes were inserted in the solution. A glassy carbon rod (Metrohm) and a saturated calomel electrode (SCE) (Radiometer analytic) were used as counter-electrode and reference electrode, respectively, while the stainless steel meshes were used as working electrode. The three electrodes were connected to an Autolab potentiostat of Metrohm. The smooth polymer films were electrodeposited at constant potential (E = 0.77 V versus SCE) and using a low deposition charge (Qs = 5 mC cm^{-2}).

The second steps consisted in the electropolymerization of the ProDOT derivatives around the polypyrrole-coated stainless steel meshes. 0.01 M of ProDOT-*n*-H_4 or ProDOT-*br*-H_4 were put in an anhydrous acetonitrile solution containing 0.1 M of tetrabutylammonium perchlorate. After degassing under argon, structured polymer films were electrodeposited by cyclic voltammetry between -1 V and 1.45 V for ProDOT-*n*-H_4 and 1.47 V for ProDOT-*br*-H_4 and at a scan rate of 20 mV s^{-1}. Various deposition scans (1, 3, 5 and 10 scans) were realized in order to study the effect of the polymer growth on the surface properties.

2.2 Surface characterization

The apparent and dynamic contact angles were obtained with a DSA30 goniometer of Krüss using liquids of various surface tension. The apparent contact angles were obtained using the sessile drop method. The dynamic contact angles were obtained with the tilted-drop method. In this method, a 6 μL droplet was deposited and the surface was inclined until the droplet rolls of the surface. The maximum surface inclination in called sliding or tilting angle (α). The advanced and receding contact angles and as a consequence the hysteresis are determined just before the droplet rolls off the surface. The SEM analyses were performed using a 6700F microscope of JEOL.

3. Results and discussion

3.1 Polymer growth

The polymer growth on the stainless steel meshes were studied by SEM analyses. Fig. 1 shows examples of SEM images after 3 deposition scans. The two monomers gave rise to the extremely homogeneous formation of nanofibers only around the mesh wires. Indeed, it is extremely important to keep the holes free because they are important for the surface wettability.[23] The shape of PProDOT-*n*-H_4 and PProDOT-*br*-H_4 nanofibers was not exactly the same and PProDOT-*br*-H_4 nanofibers were close to nanoneedles. Moreover, the porosity between the nanofibers is higher with PProDOT-*br*-H_4 (Fig. 1b) than with PProDOT-*n*-H_4 (Fig. 1e). The increase in the number of scans induced an increase in the number of polymer fibers around the mesh, as shown in Fig. 2, and as a consequence a decrease in the porosity between the fibers. The groups of Jiang[30] and Yu[31] previously the possibility to induce the elaboration of conducting polymer nanofibers using porous anodic aluminum oxide membranes as templates. The underwater oleophobicity could be controlled by varying the electrochemical potential,[30] the length and the nature of the substituent.[31]

The wettability of the meshes was investigated using liquids of various surface tension (γ_{LV}) in order to determine the liquids able to penetrate throughout the meshes: water (γ_{LV} = 72.8 mN m^{-1}), ethylene glycol (47.3 mN m^{-1}), sunflower oil (31 mN m^{-1}), hexadecane (27.6 mN m^{-1}), dodecane (25.3 mN m^{-1}), decane (23.8 mN m^{-1}), octane (21.6 mN m^{-1}) and hexane (18.4 mN m^{-1}). Fig. 3 gathers the apparent contact angle (θ) as a function γ_{LV} and the number of deposition scans, for the two polymers. Superhydrophobic properties were obtained whatever the polymer and the number of deposition scans (from 1 to 10).

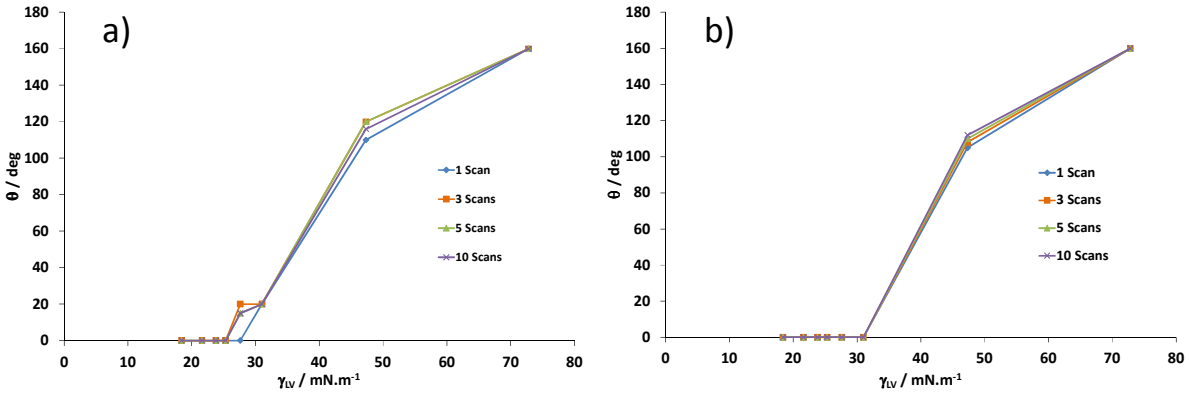

Fig. 3 Apparent contact angle as a function of liquid surface tension (γ_{LV}) and the number of deposition scans for (a) PProDOT-*n*-H_4 and (b) PProDOT-*br*-H_4 electrodeposited on stainless steel meshes.

This is an important result in order to reduce the deposition time. Moreover, dynamic contact angle measurements showed also ultra-low hysteresis and sliding angles (< 3°). Indeed, it is extremely important for oil/water separation to have superhydrophobic properties with ultra-low hysteresis in order to enhance the separation efficiency.

In terms of superoleophilicity, PProDOT-*br*-H_4 displayed a total wetting (θ = 0° for all the oils) and an extremely fast penetration of all the oils tested in our experiments (Fig. 3b). Indeed, a shoulder was observed for PProDOT-*n*-H_4 (Fig. 3a) for 25 < γ_{LV} < 31 mN m^{-1}. This shoulder may be due to the differences of porosity between the nanofibers as the number of scans changes. This shoulder was not observed with PProDOT-*br*-H_4 because the porosity between the nanofibers is higher. The results can be explain with the Wenzel and the Cassie-Baxter equations.[6-7] When a liquid droplet follows the Wenzel equation[6] ($\cos\theta = r\cos\theta^Y$ where r is a roughness parameter and θ^Y is the Young angle[32] of the corresponding smooth surface), it is in full contact with the surface leading to an increase in the solid-liquid interface by the surface roughness. In the case of meshes, the liquid droplet do not penetrate the mesh if $\theta^Y > 0°$ and reversely. This equation can lead to superhydrophobic properties if $\theta^Y_w > 90°$ but with high water adhesion due to the increase in the solid-liquid interface. It is also possible to reach superhydrophilic properties if $\theta^Y_w < 90°$ or superhydrophilic properties if $\theta^Y_{oils} < 90°$. The Cassie-Baxter equation[7] can predict superhydrophobic properties and even superoleophobic properties whatever θ^Y_w or θ^Y_{oils}, respectively. When a droplet follows the Cassie-Baxter equation, the surface porosity induces the formation of a composite interface made of solid-liquid and liquid-vapor interfaces. As described by Marmur,[33-34] the Cassie-Baxter equation can be: $\cos\theta = r_f f\cos\theta^Y + f - 1$ where r_f is roughness ratio of the wet surface, f is the solid fraction and (1 – f) is the air fraction. Superhydrophobic properties but with ultra-low hysteresis can be obtained due to the increase in the liquid-vapor interface.

Here, the presence of hydrocarbon chains, which are intrinsically hydrophobic and oleophilic favors the Cassie-Baxter state with water and the Wenzel state with oils (Fig. 4). Moreover, the microporosity of the mesh and the nanoporosity between the nanofibers enhance both the superhydrophobic and superoleophilic properties. Indeed, as shown by the group of Jiang, the stability of the meniscus of the liquid between two adjacent mesh wires is very important to predict superhydrophobic and superoleophilic properties.[35] The liquid will not penetrate throughout the mesh if the hydrostatic pressure $\Delta P = 2\gamma_{LV}/R = -l\gamma_{LV}\cos(\theta_A)/A$ where R is the radius of the meniscus, A is the cross-sectional area of the pore, l is the circumference of the pores and θ_A is the advancing contact angle of the liquid. When $\theta_A > 90°$, the liquid will not penetrate due to a negative capillary effect ($\Delta P > 0$) and reversely. Hence, the permeation is highly dependent on the mesh opening, the presence of nanostructures around the mesh wires and also on the liquid surface tension.

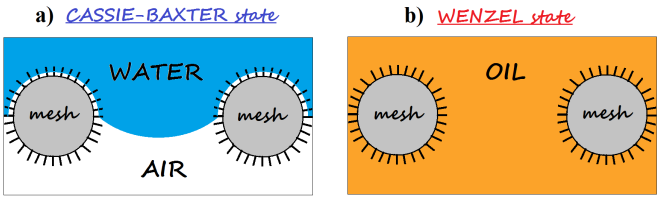

Fig. 4 Schematic representation of nanostructured stainless steel meshes with (a) repellency of water in the Cassie-Baxter state and (b) penetration of oils in the Wenzel state.

4. Conclusions

Here, we have showed the possibility produce homogeneous growth of nanofibers on stainless steel meshes, by electrodeposition of poly(3,4-propylenedioxythiophene) bearing two linear or branched alkyl chains, in order to produce superhydrophobic and superoleophilic properties. The polymers were deposited by cyclic voltammetry and using various number of deposition cycles. We have demonstrated that the highest properties were obtained with the branched alkyl chains independently of the number of deposition scans (from 1 to 10). These meshes could be used for oil/water separation.

Notes and references

Univ. Nice Sophia Antipolis, LPMC, UMR 7336, CNRS, Parc Valrose, 06100 Nice, France
Fax: (+33)4-92-07-61-56; Tel: (+33)4-92-07-61-59;
E-mail:Frederic.GUITTARD@unice.fr

1 H. Bellanger, T. Darmanin, E. Taffin de Givenchy and F. Guittard, *Chem. Rev.*, 2014, **114**, 2694.
2 E. Bormashenko, *Adv. Colloid Interface Sci.*, DOI: 10.1016/j.cis.2014.02.009.
3 T. Darmanin and F. Guittard, *J. Mater. Chem. A*, 2014, **2**, 16319.
4 M. Liu, Y. Zheng, J. Zhai and L. Jiang, *Acc. Chem. Res.*, 2010, **43**, 368.
5 X. J. Feng and L. Jiang, *Adv. Mater.*, 2006, **18**, 3063.
6 R. N. Wenzel, *Ind. Eng. Chem.*, 1936, **28**, 988.
7 A. B. D. Cassie and S. Baxter, *Trans. Faraday Soc.*, 1944, **40**, 546.
8 Y.Y. Yan, N. Gao and W. Barthlott, *Adv. Colloid Interface Sci.*, 2011, **169**, 80.
9 S. S. Latthe, A. B. Gurav, C. S. Maruti and R. S. Vhatkar, *J. Surf. Eng. Mater. Adv. Technol.*, 2012, **2**, 76.
10 T. Darmanin and F. Guittard, *Prog. Polym. Sci.*, 2014, **39**, 656.
11 Y.-Z. Long, M.-M. Li, C. Gu, M. Wan, J.-L. Duvail, Z. Liu and Z. Fan, *Prog. Polym. Sci.*, 2011, **36**, 1415.
12 C. Li, H. Bai and G. Shi, *Chem. Soc. Rev.*, 2009, **38**, 2397.
13 L. Xu, Z. Chen, W. Chen, A. Mulchandani and Y. Yan, *Macromol. Rapid Commun.*, 2008, **29**, 832.
14 H. Yan, K. Kurogi, H. Mayama and K. Tsujii, *Angew. Chem., Int. Ed.*, 2005, **44**, 3453.
15 T. Darmanin and F. Guittard, *J. Am. Chem. Soc.*, 2011, **133**, 15627.
16 S. Taleb, T. Darmanin and F. Guittard, *ACS Appl. Mater. Interfaces*, 2014, **6**, 7953.
17 T. Darmanin, C. Mortier and F. Guittard, *Adv. Mater. Interfaces*, 2014, **1**, 1300094/1.
18 S.-C. Luo, J. Sekine, B. Zhu, H. Zhao, A. Nakao and H.-h. Yu, *ACS Nano*, 2012, **6**, 3018.
19 J. El-Maiss, T. Darmanin and F. Guittard, *J. Mater. Sci.*, 2014, **49**, 7760.
20 T. Darmanin, C. Mortier, J. Eastoe, M. Sagisaka and F. Guittard, *RSC Adv.*, 2014, 4, 35708.
21 C. Mortier, T. Darmanin and F. Guittard, *ChemPlusChem*, DOI: 10.1002/cplu.201402187R1.
22 T. Darmanin, J. Tarrade, E. Celia and F. Guittard, *J. Phys. Chem. C*, 2014, **118**, 2052.
23 T. Darmanin, J. Tarrade, E. Celia, H. Bellanger and F. Guittard, *ChemPlusChem*, 2014, **79**, 382.
24 T. An, S. J. Cho, W. Choi, J. H. Kim, S. T. Lim and G. Lim, *Soft Matter*, 2011, **7**, 9867.
25 D. Tian, X. Zhang, X. Wang, J. Zhai and L. Jiang, *Phys. Chem. Chem. Phys.*, 2011, **13**, 14606.
26 Z. Cheng, M. Du, K. Fu, N. Zhang and K. Sun, *ACS Appl. Mater. Interfaces*, 2012, **4**, 5826.
27 M. Liu, S. Wang, Z. Wei, Y. Song and L. Jiang, *Adv. Mater.*, 2009, **21**, 665.
28 X. Liu, J. Zhou, Z. Xue, J. Gao, J. Meng, S. Wang and L. Jiang, *Adv. Mater.*, 2012, **24**, 3401.
29 J. Yang, Z. Zhang, X. Xu, X. Zhu, X. Men and X. Zhou, *J. Mater. Chem.*, 2012, **22**, 2834.
30 M. Liu, X. Liu, C. Ding, Z. Wei, Y. Zhu and L. Jiang, *Soft Matter*, 2011, **7**, 4163.
31 H.-A. Lin, S.-C. Luo, B. Zhu, C. Chen, Y. Yamashita and H.-h Yu, *Adv. Funct. Mater.*, 2013, **23**, 3212.
32 T. Young, *Phil. Trans. R. Soc. London*, 1805, **95**, 65.
33 a) A. Marmur, *Soft Matter*, 2012, **8**, 6867; b) A. Marmur, *Soft Matter*, 2013, **9**, 7900; b) A. Marmur, *Langmuir*, 2003, **19**, 8343.
34 A. Marmur, *Langmuir*, 2008, **24**, 7573.
35 D. Tian, X. Zhang, X. Wang, J. Zhai and L. Jiang, *Phys. Chem. Chem. Phys.*, 2011, **13**, 14606.